Joint Energy Dispatch and Unit Commitment in Microgrids Based on Deep Reinforcement Learning

Jiaju Qi, Lei Lei, *Senior Member, IEEE*, Kan Zheng, *Senior Member, IEEE*, Simon X. Yang, *Senior Member, IEEE*

arXiv:2206.01663v1 [cs.LG] 3 Jun 2022

***Abstract*—Nowadays, the application of microgrids (MG) with renewable energy is becoming more and more extensive, which creates a strong need for dynamic energy management. In this paper, deep reinforcement learning (DRL) is applied to learn an optimal policy for making joint energy dispatch (ED) and unit commitment (UC) decisions in an isolated MG, with the aim for reducing the total power generation cost on the premise of ensuring the supply-demand balance. In order to overcome the challenge of discrete-continuous hybrid action space due to joint ED and UC, we propose a DRL algorithm, i.e., the hybrid action finite-horizon DDPG (HAFH-DDPG), that seamlessly integrates two classical DRL algorithms, i.e., deep Q-network (DQN) and deep deterministic policy gradient (DDPG), based on a finite-horizon dynamic programming (DP) framework. Moreover, a diesel generator (DG) selection strategy is presented to support a simplified action space for reducing the computation complexity of this algorithm. Finally, the effectiveness of our proposed algorithm is verified through comparison with several baseline algorithms by experiments with real-world data set.**

***Index Terms*—Microgrid; Deep Reinforcement Learning; Energy Management**

I. Introduction

Microgrids (MGs) are small-scale low voltage distribution networks comprising various distributed generators, storage devices and controllable loads that can operate either interconnected or isolated from the main distribution grid as a controlled entity. Energy management is a hot research topic in MG, which can effectively coordinate the energy sharing and trading among all available energy resources, and supply loads economically in all the conditions for the reliable, secure, and efficient operation of the power system [1]. With the development of technology, the growing capacity for renewable energy sources (RES) such as wind and solar units has strongly augmented the levels of variability and uncertainty in the MG system, making the optimization of energy management a large-scale, non-convex, stochastic optimization problem [2]. Energy management in MG includes several typical functions, such as unit commitment (UC), energy dispatch (ED) [3], energy trading [4] and demand response [5].

In this paper, we mainly focus on UC and ED. As two important functions of energy management, they both play a significant role in MG. UC aims at minimizing the total cost of power generation in a specific period, by defining an optimal schedule to open or close each generating unit of the power system, subject to a given load forecast and constraints [6]; while ED aims to enhance the dispatch flexibility and reduce the cost by allocating the capacity of each generating unit. The goal behind both UC and ED is to balance demand with production while optimizing resources and costs. While there have been many traditional algorithms to solve the UC and ED problems in the past, they do not work well in face of uncertainty in MG, especially involving RES. Therefore, how to address the uncertainty in MG has aroused a widely increasing concern with researchers.

In MGs, intelligent energy management decisions can be made by leveraging machine learning techniques, especially reinforcement learning (RL). With the rapid development of deep learning, deep reinforcement learning (DRL)-based methods have been proposed and applied to handle the variability and uncertainty in RES. Compared with the traditional algorithms, DRL algorithms can learn the optimal control policies by trial and error based on real-world data [7]. Thus, DRL methods do not require rigorous mathematical models for RES and load consumption [8], [19]. Moreover, the powerful deep neural networks (DNNs) in the DRL algorithms make it possible to learn and fit complex patterns better. Finally, the computational complexity of DRL algorithms is very low during the deployment phase. It is easy for DRL methods to solve large-scale optimization problems in real-time [2] after training the DNNs, since only the forward propagation in the networks is involved [8], [20], [21].

There are several major categories of DRL algorithms applied in the energy management of MG, e.g., value-based methods such as deep Q-network (DQN) and actor-critic methods such as deep deterministic policy gradient (DDPG). However, when both UC and ED are taken into account in the system model, DRL algorithms become extremely complex due to the *discrete-continuous hybrid action space*. In this paper, we propose an advanced DRL algorithm to handle the issue of joint UC and ED, which has not been adequately addressed in existing works.

A. Related Works

In general, UC and ED are NP-hard optimization problems [9]. The mixed integer linear programming (MILP) approach has been a practical and efficient methodology that is widely applied since proposed in the 1970s [10]. However, it is not very effective when addressing the challenge of uncertainty. Note that the problems of UC and ED can be modeled as the sequential stochastic decision problem, and different research communities have addressed the problem from the perspectives of optimization, control and RL [11]. Stochastic programming (SP) is a renowned optimization technique to offer modeling and solution techniques for solving system with uncertainty [12], [13], where multi-stage models are proposed in [14]. Some works of multi-stage SP adopted scenario trees to model

the demand and unit failure uncertainties [15], [16], as well as fuel and electricity uncertainties [17]. Model predictive control (MPC), as an advanced method of optimal control, is known as an on-line closed-loop method that mitigates the issue of variability and uncertainty, and its response to large disturbances is improved when combined with stochastic methods [18].

As a promising branch of RL, DRL has been adopted for the energy management of MG [22]–[24]. Franois et al. presented a value-based model to efficiently operate the storage devices in a MG considering the uncertainty of the future electricity consumption and PV production [25]. Ji et al. directly adopted DQN to find the most cost-effective generation schedules of the MG by taking full advantage of the energy storage systems [26]. This DQN algorithm achieved the real-time dispatch of the diesel generators (DGs) and energy storage systems (ESS), which did not require an explicit model or a predictor. Wei et al. adpoted DDPG to determine the optimal reclosing time and block the power transfer [27]. Their proposed strategy could minimize the cyber-attack impacts under different scenarios. In [28], Lei et al. proposed new DRL algorithms, i.e., finite-horizon DDPG (FH-DDPG) and finite-horizon RDPG (FH-RDPG), to solve the ED problem in MG. The algorithms could effectively address the instability problem, finite-horizon setting and partial observable problem in isolated MG systems and achieve better performance than other baseline DRL methods. Besides, different from the above value-based or actor-critic methods, Huang et al. adopted a newly developed MB-DRL algorithm, namely MuZero, to perform online optimization of the MG under uncertainties [29], which combined a Monte-Carlo tree search method with the neural network model.

However, there are few studies that consider the joint optimization of UC and ED. Actually, in many common situations, in order to achieve minimum costs, system operators (SO) first determine generating units ON / OFF statuses and production capacities based on forecast values and technical constraints of each unit. Afterwards, a re-dispatch is carried out in real-time to adjust the difference between the real demand and expected output. Therefore, in [30], a two-stage MPC model was proposed to achieve UC and improve ED jointly, which enabled a cost-efficient operation and guaranteed an uninterrupted power supply. The two optimization layers consisted of an optimal control problem for the calculation of the power dispatch and a boundary value problem (BVP) for the adjustment of the DG start/stop time.

The joint optimization of UC and ED poses an important challenge for DRL-based solutions. Classical DQN or DDPG models are not suitable to handle the induced discrete-continuous hybrid action space. Previous works in DRL either approximate the hybrid space by discretization, or relax it into a continuous set. For example, Hausknecht et al. presented a successful extension of DDPG for parameterized action space [31]. This algorithm regarded both continuous and discrete actions as an integrated parameterized action space and executed a specific continuous action according to corresponding discrete values, which means the computations to solve complex discrete-continuous hybrid action space are avoided. In addition, Xiong et al. proposed a parametrized deep Q-network (P-DQN) framework for the hybrid action space without approximation or relaxation [32]. P-DQN combined the characteristics of both DQN (dealing with discrete action space) and DDPG (dealing with continuous action space) by seamlessly integrating them. Inspired by this research, we design a DRL algorithm to jointly optimize UC and ED.

B. Contributions

The main contributions of this paper are summarized as follows.

1) A novel DRL algorithm, i.e., *hybrid action finite-horizon DDPG (HAFH-DDPG)*, is proposed with the aim for deriving the joint UC and ED policy. The integration of DDPG and DQN characteristics enables our algorithm to have great advantages in dealing with the discrete-continuous hybrid action space in the DRL model. Moreover, the finite-horizon value iteration framework improves the stability of the DRL algorithm in the finite-horizon setting. The proposed algorithm fills in the gap of applying DRL methods for joint UC and ED in MG.
2) To reduce the computation complexity of HAFH-DDPG, we present a simplified action space based on a proposed DG selection strategy. We prove that this simplification does not come at the expense of performance erosion, as the proposed algorithm with the simplified action space achieves the same performance as original algorithm.

The rest of the paper is organized as follows. The framework of our MG system model are briefly introduced in Section II. Section III falls into the description of our MDP model. The design of HAFH-DDPG algorithm is presented in Section IV. In section V, the experiments are conducted to verify the efficiency of our algorithm. Finally, the conclusion is drawn in Section VI.

II. System Model

The isolated MG system considered in this paper can be divided into five parts, i.e., the controllable generation units (i.e., DGs), uncontrollable generation units (i.e., photovoltaic cell (PV)), energy storage devices (i.e., battery storage), loads, and SO (i.e., DRL-based intelligent server), to perform UC and ED. PV and DGs can supply electric power to the loads. DGs usually act as the main power source and incur a high operation cost mainly due to the fuel consumption. PV offers a clean source of power and largely reduces the operation cost, but it brings additional uncertainty into the MG due to the intermittency and unpredictability of renewables. Battery, as a backup force, provides flexible adjustment means for MG. The extra energy can be stored in the battery for use in case there is insufficient electric power generation capacity.

The intra-day operation of our MG system model is divided into T time steps, indexed by $\{1, \cdots, T\}$. The interval of each time step is denoted as Δt.

A. Diesel Generator Model

Consider there are D switchable DGs in our system model, i.e., $\mathrm{DG}_1, \cdots, \mathrm{DG}_D$, where $D > 1$. The status of DGs'

switches is a set of boolean variables. Let $B_t^{\mathrm{DG}_d}$ denote the ON/OFF status of DG_d, $\forall d \in \{1, \cdots, D\}$, *at the beginning* of time step t, where 1 stands for ON, while 0 stands for OFF.

Let $U_t^{\mathrm{DG}_d}$ denote the UC decision of DG_d made at time step t, where 1 stands for ON, while 0 stands for OFF. After the UC decision $U_t^{\mathrm{DG}_d}$ is made at time step t, the ON/OFF status of DG_d will be set accordingly for the rest of the time step. Note that the ON/OFF status $B_t^{\mathrm{DG}_d}$ at the beginning of time step t is actually the same as the UC decision $U_{t-1}^{\mathrm{DG}_d}$ at the previous time step $t-1$. Therefore, we have the relationship between the two variables, i.e.,

$$U_{t-1}^{\mathrm{DG}_d} = B_t^{\mathrm{DG}_d}. \tag{1}$$

At time step t, let $P_t^{\mathrm{DG}_d}$ denote the output power of the d-th DG DG_d, $\forall d \in \{1, \cdots, D\}$, which also represents the ED decision in the MG system. When a DG is switched off, its output power is 0. Otherwise, its output power can be any real number from the minimum power limit to the maximum power limit. Thus, the allowable power generation of DGs can be described as

$$\begin{array}{ll} P_t^{\mathrm{DG}_d} = 0, & \text{if } U_t^{\mathrm{DG}_d} = 0 \\ P_{\min}^{\mathrm{DG}} \leq P_t^{\mathrm{DG}_d} \leq P_{\max}^{\mathrm{DG}} & \text{if } U_t^{\mathrm{DG}_d} = 1 \end{array}, \tag{2}$$

where $P_{\min}^{\mathrm{DG}}$ and $P_{\max}^{\mathrm{DG}}$ are the minimum and maximum output power constraints of a DG, respectively.

B. Battery Model

Let E_t be the state of charge (SoC) of the battery at time step t. E_t is constrained by the maximum energy level $E_{\max}$ and the minimum energy level $E_{\min}$ of the battery, i.e.,

$$E_{\min} \leqslant E_t \leqslant E_{\max}. \tag{3}$$

The SoC of battery E_{t+1} at time step $t+1$ can be calculated based on the SoC state E_t at time step t as

$$E_{t+1} = E_t + \eta_{\mathrm{ch}} u_t P_t^{\mathrm{E}} \Delta t - (1-u_t) P_t^{\mathrm{E}} \Delta t / \eta_{\mathrm{dis}}, \tag{4}$$

where η_{ch} and η_{dis} denote the charging and discharging efficiencies of the battery, respectively. P_t^{E} indicates the charging or discharging power of the battery, and u_t denotes charging or discharging status, which is 0 if battery is discharging and 1 otherwise. In order to determine P_t^{E} and u_t, a variable δ_t is defined to represent the surplus of generating capacity at time step t, i.e.,

$$\delta_t = \sum_{d=1}^{D} P_t^{\mathrm{DG}_d} + P_t^{\mathrm{PV}} - P_t^{\mathrm{L}}, \tag{5}$$

where P_t^{PV} is the output power of PV and P_t^{L} is the load consumption at time step t. When a surplus is generated, i.e., $\delta_t > 0$, the excess power is stored in the battery. At this point, the battery is in the charging status. On the contrary, when the power generation of PV and DGs is insufficient, i.e., $\delta_t < 0$, the battery is in the discharge state. In this way, u_t can be defined based on δ_t, which is set as follows,

$$u_t = \begin{cases} 0, & \text{if } \delta_t < 0 \\ 1, & \text{otherwise} \end{cases}. \tag{6}$$

To derive P_t^{E}, let $P_{\max}^{\mathrm{E}}$ be the maximum charging or discharging power of the battery. Then, the charging and discharging power limits of the battery can be calculated separately, i.e.,

$$P_{\mathrm{ch\_lim}}^{\mathrm{E}} = \min(P_{\max}^{\mathrm{E}}, (E_{\max} - E_t)/(\eta_{\mathrm{ch}} \Delta t)), \tag{7}$$

and

$$P_{\mathrm{dis\_lim}}^{\mathrm{E}} = \min(P_{\max}^{\mathrm{E}}, \eta_{\mathrm{dis}}(E_t - E_{\min})/\Delta t). \tag{8}$$

Now, P_t^{E} can be derived based on δ_t as

$$P_t^{\mathrm{E}} = \begin{cases} \min\left(-\delta_t, P_{\mathrm{dis\_lim}}^{\mathrm{E}}\right), & \text{if } \delta_t < 0 \\ \min\left(\delta_t, P_{\mathrm{ch\_lim}}^{\mathrm{E}}\right), & \text{otherwise} \end{cases}. \tag{9}$$

To elaborate on (9), if $\delta_t > 0$, the power generation is larger than demand, and the excessive power will be charged to the battery. However, if $\delta_t > P_{\mathrm{ch\_lim}}^{\mathrm{E}}$, the excessive power beyond the charging capability of the battery will go to load bank, which will be lost or generation will be curtailed. If $\delta_t < 0$, the generation is smaller than demand, the battery needs to be discharged to provide the lacked power. However, if $\delta_t < P_{\mathrm{dis\_lim}}^{\mathrm{E}}$, even the battery cannot provide enough power, which will result in some of the loads unserved. In summary, by calculating P_t^{E} with (9) and u_t with (6), the SoC state E_t can be derived according to the iterative relations in (4) at every time step.

III. MDP Model

In this section, we shall formulate a Markov decision process (MDP) model based on which the strategic UC and ED decisions using RL can be made. The objective of our MDP model is to minimize the total cost and ensure the supply-demand balance, where the uncertainty of both fluctuating loads and stochastic generation of PV are taken into account.

A. State

We define the system state S_t at time step t, $\forall t \in \{1, \cdots, T\}$, by several components, i.e., $S_t = \left(P_t^{\mathrm{L}}, P_t^{\mathrm{PV}}, E_t\right)$. Let $\mathcal{S}$ denote the state space, which consists of three components, i.e., $\mathcal{S} = \mathcal{P}^{\mathrm{L}} \times \mathcal{P}^{\mathrm{PV}} \times \mathcal{E}$, where $\mathcal{P}^{\mathrm{L}}$, $\mathcal{P}^{\mathrm{PV}}$, and $\mathcal{E}$ denote the state space of load, PV, and battery, respectively. In addition, there exists constraints in these state spaces, i.e.,

$$\mathcal{P}^{\mathrm{L}} = \left[0, P_{\max}^{\mathrm{L}}\right], \mathcal{P}^{\mathrm{PV}} = \left[0, P_{\max}^{\mathrm{PV}}\right], \mathcal{E} = \left[E_{\min}, E_{\max}\right], \tag{10}$$

where $P_{\max}^{\mathrm{L}}$ and $P_{\max}^{\mathrm{PV}}$ denote the maximum load power and PV power, respectively, which are derived from the data set.

B. Action

We define the action A_t at time step $t \in \{1, \cdots, T\}$, by two components, i.e, $A_t = \left(A_t^{\mathrm{UC}}, A_t^{\mathrm{ED}}\right)$. A_t^{UC} denotes the UC action at time step t, i.e., how to set DGs' switches, which is a vector of *discrete* variable. Therefore, A_t^{UC} can be written as $A_t^{\mathrm{UC}} = \{U_t^{\mathrm{DG}_d}\}_{d=1}^{D}, \forall d \in \{1, 2, \cdots D\}$. A_t^{ED} represents the ED action to dispatch generation power to each DG, which is a vector of *continuous* variable, i.e., $A_t^{\mathrm{ED}} = \{P_t^{\mathrm{DG}_d}\}_{d=1}^{D}, \forall d \in \{1, 2, \cdots D\}$.

The action space can be described as $\mathcal{A}$, which consists of two components, i.e., the UC action space $\mathcal{A}^{\mathrm{UC}}$ and the ED action space $\mathcal{A}^{\mathrm{ED}}$. Thus, $\mathcal{A}$ is derived as $\mathcal{A} = \mathcal{A}^{\mathrm{UC}} \times \mathcal{A}^{\mathrm{ED}}$.

Considering that there are D DGs in the model, the size of $\mathcal{A}^{\mathrm{UC}}$ is 2^D. $\mathcal{A}^{\mathrm{UC}}$ is D permutations of 0 and 1. Let a_k^{UC} denote the k-th action in the UC action space $\mathcal{A}^{\mathrm{UC}}$, where $k \in \left\{1, ..., 2^D\right\}$ is the index of the UC action. Since there is a one-to-one correspondence between a_k^{UC} and k, we substitute k for a_k^{UC} for convenience in the rest of this paper.

The ED action space $\mathcal{A}^{\mathrm{ED}}$ is

$$\mathcal{A}^{\mathrm{ED}} = \{0\} \cup \left[P_{\min}^{\mathrm{DG}}, P_{\max}^{\mathrm{DG}}\right]. \tag{11}$$

According to (2), $\mathcal{A}^{\mathrm{ED}}$ is related to the UC action k. Therefore, let $\mathcal{A}_k^{\mathrm{ED}}$ denote the ED action space corresponding to the chosen UC action k. Let a_k^{ED} denote an action belonging to the ED action space $\mathcal{A}_k^{\mathrm{ED}}$, i.e., $a_k^{\mathrm{ED}} \in \mathcal{A}_k^{\mathrm{ED}}$.

C. Reward Function

The optimization objective in the MG system is to minimize the total operation cost (TOC) within the considered time horizon, i.e., one day. In our MG system model, the TOC consists of four parts, i.e., cost of supply-demand balance, DG power generation cost, start-up cost, and running cost. Therefore, we define the reward function as

$$r(S_t, A_t) = -\left(\sum_{d=1}^{D}(c_t^{\mathrm{DG}_d} + c_t^{\mathrm{S\_DG}_d} + c_t^{\mathrm{R\_DG}_d}) + c_t^{\mathrm{US}}\right). \tag{12}$$

Firstly, c_t^{US} is the cost of supply-demand balance, which represents the cost of aggregated unserved or lost active power, i.e.,

$$c_t^{\mathrm{US}} = \begin{cases} k_1(\delta_t - P_{\mathrm{ch\_lim}}^{\mathrm{E}})\Delta t, & \text{if } \delta_t > P_{\mathrm{ch\_lim}}^{\mathrm{E}} \\ -k_2(\delta_t + P_{\mathrm{dis\_lim}}^{\mathrm{E}})\Delta t, & \text{if } \delta_t < -P_{\mathrm{dis\_lim}}^{\mathrm{E}} \\ 0, & \text{otherwise} \end{cases}, \tag{13}$$

where k_1 and k_2 are weights that indicate the relative importance of unserved power situation and lost power situation.

Let $c_t^{\mathrm{DG}_d}$ denote the power generation cost of DG_d, which can be derived by the conventional quadratic cost function

$$c_t^{\mathrm{DG}_d} = [a_d(P_t^{\mathrm{DG}_d})^2 + b_d P_t^{\mathrm{DG}_d} + c_d]\Delta t, \forall d \in \{1, \cdots, D\}, \tag{14}$$

where a_d, b_d, and c_d are positive coefficients for DG_d.

Let $c_t^{\mathrm{S\_DG}_d}$ denote the start-up cost of DG_d, which can be derived as

$$c_t^{\mathrm{S\_DG}_d} = C_{\mathrm{S}} U_t^{\mathrm{DG}_d}(1 - B_t^{\mathrm{DG}_d})\Delta t, \forall d \in \{1, \cdots, D\}, \tag{15}$$

where C_{S} represents a fixed start-up cost coefficient. It can be found that only when a DG is closed at time step $t-1$ but turned on at time step t, i.e., $B_t^{\mathrm{DG}_d} = 0$ and $U_t^{\mathrm{DG}_d} = 1$ will incur the start-up cost.

Finally, $c_t^{\mathrm{R\_DG}_d}$ denotes the running cost of DG_d, which can be derived as

$$c_t^{\mathrm{R\_DG}_d} = C_{\mathrm{R}} U_t^{\mathrm{DG}_d}\Delta t, \forall d \in \{1, \cdots, D\}, \tag{16}$$

where C_{R} represents a fixed running cost coefficient. As soon as one DG is turned on, it will give rise to the running cost.

D. Transition Probability

The state transition probability $\Pr\left(s_{t+1}|s_t, a_t\right)$ is derived as

$$\begin{aligned}\Pr\left(S_{t+1}|S_t, A_t\right) = \Pr\left(P_{t+1}^{\mathrm{L}}|P_t^{\mathrm{L}}\right) \Pr\left(P_{t+1}^{\mathrm{PV}}|P_t^{\mathrm{PV}}\right) \\ \Pr\left(E_{t+1}|E_t, A_t^{\mathrm{ED}}\right) \Pr\left(B_{t+1}|B_t, A_t^{\mathrm{UC}}\right),\end{aligned} \tag{17}$$

where the transition probabilities of the load power demands $\Pr\left(P_{t+1}^{\mathrm{L}}|P_t^{\mathrm{L}}\right)$ and PV power outputs $\Pr\left(P_{t+1}^{\mathrm{PV}}|P_t^{\mathrm{PV}}\right)$ are not available, but samples of the trajectory can be obtained from the real-world data. The transition probability of the SoC $\Pr\left(E_{t+1}|E_t, A_t^{\mathrm{ED}}\right)$ can be calculated through (4). The last transition probability $\Pr\left(B_{t+1}|B_t, A_t^{\mathrm{UC}}\right)$ is for the switching state, which can be easily inferred from (1). It can be found that the switching state of DG_d at the next time step $t+1$ is the same as the UC action $U_t^{\mathrm{DG}_d}$.

IV. DRL Solution

A. Dealing with the hybrid action space

Since the action A_t in our MDP model includes both continuous and discrete variables, the action space $\mathcal{A}$ is a discrete-continuous hybrid space, while most of the existing DRL algorithms require either a discrete space or a continuous space. Inspired by the P-DQN algorithm in [32], we break the optimization problem down into two steps and design a new algorithm to solve this problem.

Firstly, our optimization objective is to find the policy π^* that can maximize the action value $Q\left(S_t, k, a_k^{\mathrm{ED}}\right)$, i.e.,

$$\pi^*(S_t) = \left(k^*, a_k^{\mathrm{ED}^*}\right) = \underset{k\in\{1,...,2^D\}}{\arg\max} \underset{a_k^{\mathrm{ED}}\in\mathcal{A}_k^{\mathrm{ED}}}{\arg\max} Q\left(S_t, k, a_k^{\mathrm{ED}}\right), \tag{18}$$

where k^* and $a_k^{\mathrm{ED}^*}$ denote the optimal UC action and ED action, respectively.

For the discrete UC action k, there are 2^D choices. For any given UC action $k \in \left\{1, ..., 2^D\right\}$, we are able to select the best ED action $a_k^{\mathrm{ED}^*}$ from the ED action space $\mathcal{A}_k^{\mathrm{ED}}$ by solving

$$a_k^{\mathrm{ED}^*} = \underset{a_k^{\mathrm{ED}}\in\mathcal{A}_k^{\mathrm{ED}}}{\arg\max} Q\left(S_t, k, a_k^{\mathrm{ED}}\right), \forall k \in \left\{1, ..., 2^D\right\}. \tag{19}$$

However, as a_k^{ED} is a continuous variable, it should be noted that (19) cannot be solved straightforwardly by some classical value-based algorithms, such as Q-learning and DQN [33]. Therefore, our algorithm adopts the actor-critic framework to calculate the optimal ED action $a_k^{\mathrm{ED}^*}$.

Specifically, for a given UC action $k, \forall k \in \left\{1, ..., 2^D\right\}$, an actor network $\mu_k\left(\cdot;\theta\right) : \mathcal{S} \rightarrow \mathcal{A}_k^{\mathrm{ED}}$ is introduced to approximate the optimal ED action $a_k^{\mathrm{ED}^*}$ from the continuous space $\mathcal{A}_k^{\mathrm{ED}}$ such that

$$a_k^{\mathrm{ED}^*} \approx \mu_k\left(S_t;\theta\right), \tag{20}$$

where θ is the weights of μ_k. Correspondingly, a critic network $\lambda_k\left(\cdot;w\right)$ is applied to evaluate the ED action $a_k^{\mathrm{ED}^*}$ and approximate the action value $Q\left(S_t, k, a_k^{\mathrm{ED}^*}\right)$, i.e.,

$$Q\left(S_t, k, a_k^{\mathrm{ED}^*}\right) \approx \lambda_k\left(S_t, a_k^{\mathrm{ED}^*}; w\right), \tag{21}$$

where w denotes the weights of λ_k.

Once the optimal ED action $a_k^{\mathrm{ED}^*}$ for all the UC action $k, \forall k \in \left\{1, ..., 2^D\right\}$, are derived, we could choose the optimal

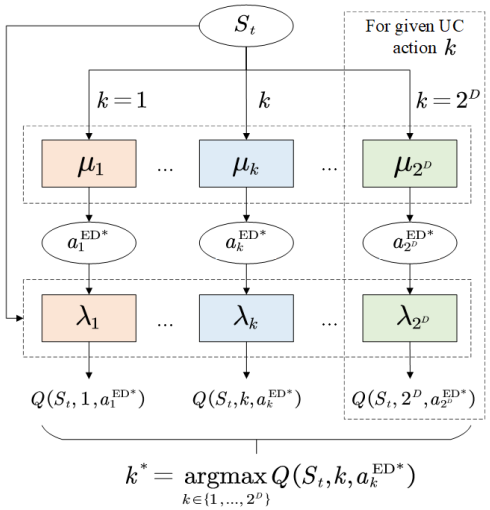

Fig. 1: The neural network framework of HAFH-DDPG.

UC action k^* from the 2^D-dimensional discrete UC action space. The above action value $Q\left(S_t,k,a_k^{\mathrm{ED}^*}\right)$ given by the critic network λ_k can be used to evaluate the UC action k when the corresponding optimal ED action $a_k^{\mathrm{ED}^*}$ is applied. We choose the UC action k with the largest action value as the optimal solution. Thus, k^* is derived as

$$k^* = \underset{k\in\{1,\ldots,2^D\}}{\arg\max}\ Q\left(S_t,k,a_k^{\mathrm{ED}^*}\right). \tag{22}$$

In summary, our strategy is to conduct ED action optimization by an actor-critic algorithm in the continuous space when fixing the discrete UC action at first, and then find the optimal UC action in the discrete space through the critic networks, as shown in Figure 1. In order to train the actor and critic networks, we focus on the action value function $Q\left(S_t,A_t\right)=Q\left(S_t,A_t^{\mathrm{UC}},A_t^{\mathrm{ED}}\right)$ based on the Bellman equation as

$$\begin{aligned}&Q\left(S_t,A_t^{\mathrm{UC}},A_t^{\mathrm{ED}}\right)=r(S_t,A_t^{\mathrm{UC}},A_t^{\mathrm{ED}})+\\&\underset{S_{t+1}}{\mathbb{E}}\left[\gamma\cdot\max_{k\in\{1,\ldots,2^D\}}\max_{a_k^{\mathrm{ED}}\in\mathcal{A}_k^{\mathrm{ED}}}Q\left(S_{t+1},k,a_k^{\mathrm{ED}}\right)|S_t,A_t^{\mathrm{UC}},A_t^{\mathrm{ED}}\right],\end{aligned} \tag{23}$$

where γ is the discount factor that satisfies $0\leqslant\gamma\leqslant 1$.

Thus, the loss function $L_k(w)$ of the critic network λ_k can be calculated as the mean square error, i.e.,

$$\begin{aligned}L_k(w)=&\underset{S_t\sim\rho_k^{\mu},a_k^{\mathrm{ED}}\sim\mu_k}{\mathbb{E}}\left[\left(y_{t,k}-\lambda_k\left(S_t,a_k^{\mathrm{ED}};w\right)\right)^2\right],\\&\forall k\in\left\{1,\ldots,2^D\right\},\end{aligned} \tag{24}$$

where ρ_k^{μ} denotes the discounted state visitation distribution following policy μ_k. $y_{t,k}$ denotes the target for each critic network λ_k at time step t, which is defined based on the Bellman equation in (23) as

$$\begin{aligned}y_{t,k}&=r_t+\gamma\max_{k\in\{1,\ldots,2^D\}}Q\left(S_{t+1},k,\mu_k(S_{t+1};\theta)\right)\\&\approx r_t+\gamma\max_{k\in\{1,\ldots,2^D\}}\lambda_k\left(S_{t+1},\mu_k\left(S_{t+1};\theta\right);w\right).\end{aligned} \tag{25}$$

By minimizing the loss function $L_k(w)$ via stochastic gradient descent, the weight w of λ_k can be updated at each time step by

$$\begin{aligned}w\leftarrow&w+2\beta\left(y_{t,k}-\lambda_k\left(S_t,\mu_k(S_t;\theta);w\right)\right)\\&\cdot\nabla_w\lambda_k\left(S_t,\mu_k(S_t;\theta);w\right),\end{aligned} \tag{26}$$

where β is the learning rate for updating w.

The loss function of actor network μ_k can be defined as

$$\begin{aligned}L_k\left(\theta\right)&=-\underset{S_0\sim\rho^0}{\mathbb{E}}\left[Q\left(S_0,k,\mu_k(S_t;\theta)\right)\right]\\&\approx-\underset{S_0\sim\rho^0}{\mathbb{E}}\left[\lambda_k\left(S_0,\mu_k\left(S_t;\theta\right);w\right)\right],\forall k\in\left\{1,\ldots,2^D\right\},\end{aligned} \tag{27}$$

where ρ_0 is the distribution of the initial state S_0.

μ_k can be updated according to the deterministic policy gradient theorem [34], where the deterministic policy gradient $\nabla_\theta J_k(\theta)$ is derived as

$$\begin{aligned}\nabla_\theta J_k\left(\theta\right)=\underset{S_t\sim\rho_k^{\mu}}{\mathbb{E}}\Big[&\nabla_\theta\mu_k\left(S_t;\theta\right)\\&\nabla_{a_k^{\mathrm{ED}}}\lambda_k\left(S_t,a_k^{\mathrm{ED}};w\right)|_{a_k^{\mathrm{ED}}=\mu_k(S_t;\theta)}\Big].\end{aligned} \tag{28}$$

Specifically, we use stochastic gradient decent to sample deterministic policy gradient in (28). Then, the weight θ of μ_k can be updated by

$$\theta\leftarrow\theta-\alpha\nabla_\theta\mu_k\left(S_t;\theta\right)\nabla_{a_k^{\mathrm{ED}}}\lambda_k\left(S_t,a_k^{\mathrm{ED}};w\right)|_{a_k^{\mathrm{ED}}=\mu_k(S_t;\theta)}, \tag{29}$$

where α is the learning rate for updating θ.

B. Designing the framework

As we focus on energy management within one day with T time steps, our task corresponds to a finite horizon MDP model. However, DDPG is developed for an infinite horizon setting. Note that an important difference between finite horizon and infinite horizon MDP is that the value function, i.e., critic, and the policy, i.e., actor, are normally dependent on the time steps in the former case. Therefore, we adopt the framework of FH-DDPG algorithm to design our DRL algorithm. FH-DDPG is a combination of dynamic programming and DRL, where DDPG is embedded within the framework of finite horizon value iteration. The finite horizon value iteration starts from the time step $T-1$, and uses backward induction to iteratively derive the value function and optimal policy for each time step $t\in\{T-1,T-2,...,1\}$, until it reaches the first time step $t=1$. In FH-DDPG, the DDPG algorithm is adopted to derive the value function λ_t and optimal policy μ_t. Specifically, in each time step, the DDPG algorithm is used to solve a simple one-step MDP where the target actor and critic networks, i.e., $\lambda_t^{'}$ and $\mu_t^{'}$ are fixed to be the trained actor and critic networks of the next time step, i.e., λ_{t+1} and μ_{t+1}, which greatly increases stability and performance of the algorithm. FH-DDPG has been applied in the field of smart grid in [28] and achieved good results. Therefore, this paper uses FH-DDPG as the framework to train the actors and critics and proposes the HAFH-DDPG.

Algorithm 1 describes the pseudocode of HAFH-DDPG. Note that similar to FH-DDPG, the target at time step $T-1$ is derived by the myopic policy, which is denoted as μ^{myopic}.

Algorithm 1 HAFH-DDPG algorithm

Randomly initialize actor networks $\mu_k(s;\theta_k)$ and critic networks $\lambda_k(s,a;w_k)$ with weights $\theta_k=\theta_k^0$ and $w_k=w_k^0$, respectively, where $\forall k\in\{1,...,2^D\}$. Initialize target networks $\mu_k^{'}\left(s;\theta_k^{'}\right)$ and $\lambda_k^{'}\left(s,a;w_k^{'}\right)$ with $\theta_k^{'}\leftarrow\theta_k$ and $w_k^{'}\leftarrow w_k$;
for $t=T-1,...,1$ **do**
  Initialize replay buffer $\mathcal{R}$
  Initialize a random process $\mathcal{N}$ for action exploration
  for episode $e=1,...,M$ **do**
    Receive state $S_t^{(e)}$
    $k_t^{(e)}, A_t^{\mathrm{ED}(e)}$=ACTION($S_t^{(e)}$,$\mu_k(s;\theta_k)$,$\lambda_k(s,a;w_k)$)
    Execute action and observe reward $r_t^{(e)}$ and next state $S_{t+1}^{(e)}$
    Store transition $\left(S_t^{(e)},k_t^{(e)},A_t^{\mathrm{ED}(e)},r_t^{(e)},S_{t+1}^{(e)}\right)$ into $\mathcal{R}$
    Sample a random minibatch of N transitions $\mathcal{B}=\left(S_t^{(i)},k_t^{(i)},A_t^{\mathrm{ED}(i)},r_t^{(i)},S_{t+1}^{(i)}\right)$ from $\mathcal{R}$
    if $t=T-1$ **then**
      Set the target

$$y_t^{(i)}=r_t^{(i)}+\gamma\cdot r_T\left(S_{t+1}^{(i)},\mu^{\mathrm{myopic}}\left(S_{t+1}^{(i)}\right)\right)$$

    else
      Set the target

$$y_t^{(i)}=r_t^{(i)}+\gamma\cdot\max_{k\in\{1,...,2^D\}}\lambda_k^{'}\left(S_{t+1}^{(i)},\mu_k^{'}\left(S_{t+1}^{(i)};\theta_k\right);w_k\right)$$

    end if
    UPDATE($\mathcal{B}$,$y_t^{(i)}$,$\mu_k(s;\theta_k)$,$\lambda_k(s,a;w_k)$)
  end for
end for

The main difference between FH-DDPG and HAFH-DDPG falls into the calculation of the hybrid actions and the method to update networks, which are presented by two functions separately, i.e., Algorithms 2 and 3. In the Action Calculation function, we introduce multiple actor networks to calculate the optimal ED actions for every UC action. According to (22), we choose the optimal UC action whose critic network has the largest output value and the corresponding ED action. In the Networks Updating function, in order to update the critic networks, the minibatch of transitions $\mathcal{B}$ are further divided into non-overlapping subsets according to the UC actions. The critic network λ_k is updated by a minibatch of transitions $\mathcal{H}$ in which the UC action of each transition is k. After that, the actor networks can be updated based on $\mathcal{B}$ using the sampled policy gradient.

Remark 1 (Myopic policy): In this policy, the action A_t is directly optimized by minimizing the reward function $r_t(S_t,A_t)$ without foreseeing the impact of the future rewards at each time step $t\in\{1,2,...,T\}$. In other words, the generation capacity of the DGs at each time step only meets the current load, and there is no additional generation schedule for battery charging to meet the future demand gap.

Algorithm 2 Action calculation

function ACTION($S_t^{(e)}$, $\mu_k(s;\theta_k)$, $\lambda_k(s,a;w_k)$)
  for UC action $k=1,...,2^D$ **do**
    Calculate ED action $a_k^{\mathrm{ED}*(e)}=\mu_k\left(S_t^{(e)};\theta_k\right)$
  end for
  Select UC action $k_t^{(e)}=\arg\max_{k\in\{1,...,2^D\}}\lambda_k\left(S_t^{(e)},a_k^{\mathrm{ED}*(e)};w_k\right)$
  Select ED action $A_t^{\mathrm{ED}(e)}=a_{k_t^{(e)}}^{\mathrm{ED}\,*(e)}$
  Adjust UC action $k_t^{(e)}$ according to the ϵ-greedy policy
  Adjust ED action $A_t^{\mathrm{ED}(e)}$ with exploration noise
  return $k_t^{(e)}$ and $A_t^{\mathrm{ED}(e)}$
end function

Algorithm 3 Networks updating

function UPDATE($\mathcal{B}$, $y_t^{(i)}$, $\mu_k(s;\theta_k)$, $\lambda_k(s,a;w_k)$)
  for $k=1,...,2^D$ **do**
    Sample the minibatch of transitions $\mathcal{H}=\left(S_t^{(h)},k_t^{(h)},A_t^{\mathrm{ED}(h)},r_t^{(h)},S_{t+1}^{(h)}\mid k_t^{(h)}=k\right)$ from $\mathcal{B}$ and corresponding targets $y_t^{(h)}$
    Update the critic networks by minimizing the loss:

$$L_k=\frac{1}{|\mathcal{H}|}\sum_{h\in\mathcal{H}}\left(y_t^{(h)}-\lambda_k\left(S_t^{(h)},A_t^{\mathrm{ED}(h)};w_k\right)\right)^2,$$

$$w_k\leftarrow w_k+\beta\nabla_{w_k}L_k$$

  end for
  Update the actor networks using the sampled policy gradient:

$$\nabla_{\theta_k}J_k\approx\frac{1}{|\mathcal{B}|}\sum_i\Big[\nabla_a\lambda_k(s,a;w_k)\,|_{s=S_t^{(i)},a=\mu_k\left(S_t^{(i)};\theta_k\right)}\nabla_{\theta_k}\mu_k\left(S_t^{(i)};\theta_k\right)\Big],\theta_k\leftarrow\theta_k+\alpha\nabla_{\theta_k}J_k.$$

  Update the target networks: $w_k^{'}\leftarrow w_k$, $\theta_k^{'}\leftarrow\theta_k$
  Save weight of the actor networks: $\theta_{k,t}\leftarrow\theta_k$
  Reset weight of the actor and critic networks to initial value: $\theta_k\leftarrow\theta_k^0$, $w_k\leftarrow w_k^0$
end function

C. Reducing the algorithm complexity

Note that the HAFH-DDPG algorithm requires $\left|\mathcal{A}^{\mathrm{UC}}\right|=2^D$ actor and critic networks. In order to reduce the computational complexity, we map the action space to a new space with reduced dimensionality. We consider the case when all DG parameters are identical. The new UC action space $\hat{\mathcal{A}}^{\mathrm{UC}}$ is defined as $\hat{\mathcal{A}}^{\mathrm{UC}}=\{0,1,...,D\}$, where a simplified UC action in the new space $m\in\hat{\mathcal{A}}^{\mathrm{UC}}$ corresponds to the number of DGs that are ON. Compared with $\mathcal{A}^{\mathrm{UC}}$, the size of $\hat{\mathcal{A}}^{\mathrm{UC}}$ is reduced from 2^D to $D+1$, which can in turn reduce the number of neural networks and the computation complexity.

Note that there is a one-to-many relationship between m and k. Specifically, each m corresponds to C_D^m possible UC actions k. When m DGs should be ON, the corresponding UC

actions k form a subset $\mathcal{A}_m^{\mathrm{UC}}$ within $\mathcal{A}^{\mathrm{UC}}$. In other words, $\mathcal{A}^{\mathrm{UC}}$ can be divided into $D+1$ non-overlapping subsets, i.e.,

$$\bigcup_{m=0}^{D} \mathcal{A}_m^{\mathrm{UC}} = \mathcal{A}^{\mathrm{UC}}. \tag{30}$$

In the following, we introduce a strategy that maps a simplified UC action $m \in \hat{\mathcal{A}}^{UC}$ to a unique UC action $k_m \in \mathcal{A}_m^{\mathrm{UC}}$.

DG Selection Strategy. First, a priority value is assigned for each $\mathrm{DG}_d, \forall d \in \{1, 2, ..., D\}$, so that DG_1 has the highest priority and DG_D has the lowest. If m DGs should be ON at time step t where $\forall m \in \{0, 1, ..., D\}$, the UC action under this strategy k_m should be

$$k_m = \left(\left\{ U_t^{\mathrm{DG}_d} \right\}_{d=1}^{m} = 1, \left\{ U_t^{\mathrm{DG}_d} \right\}_{d=m+1}^{D} = 0 \right). \tag{31}$$

With the above strategy, we can first map each m to k_m, and then choose the optimal m^* as

$$m^* = \arg\max_{m \in \hat{\mathcal{A}}^{\mathrm{UC}}} Q\left(S_t, k_m, a_{k_m}^{\mathrm{ED}^*}\right). \tag{32}$$

Specifically, the HAFH-DDPG algorithm given in Algorithm 1, 2, and 3 can be used to train the actor and critic networks by replacing the UC action k with the simplified UC action m. However, in the eighth line of Algorithms 1, $m_t^{(e)}$ should first be mapped to $k_t^{(e)}$ by the DG selection strategy before its execution to derive the reward and next state. Since each m corresponds to a unique k_m, the reward $r(S_t, m, a_m^{\mathrm{ED}^*})$ and transition probability $\Pr\left(S_{t+1}|S_t, m, a_m^{\mathrm{ED}^*}\right)$ can be derived by replacing m with k_m in the expressions. Finally, the optimal simplified UC action m^* is mapped to the UC action k_{m^*}.

We now provide Theorem 1 which elaborates that the two UC actions, i.e., k^* derived by (22) and k_{m^*} with m^* derived by (32), achieve the same performance. The rigorous proof is provided in Appendix A.

Theorem 1. *Suppose that all the DG parameters are identical, the MDPs with action space $\hat{\mathcal{A}}^{\mathrm{UC}}$ and $\mathcal{A}^{\mathrm{UC}}$ have the same optimal performance given that the above DG selection strategy is used to determine the m DGs that are ON, i.e.,*

$$\max_{m \in \hat{\mathcal{A}}^{\mathrm{UC}}} Q\left(S_t, k_m, a_{k_m}^{\mathrm{ED}^*}\right) = \max_{k \in \mathcal{A}^{\mathrm{UC}}} Q\left(S_t, k, a_k^{\mathrm{ED}^*}\right). \tag{33}$$

V. Experimental Results

In order to evaluate the effectiveness of the proposed HAFH-DDPG algorithm, we perform experiments based on real-world data in this section and discuss about the simulation results.

A. Experimental Setup

Several benchmark algorithms are selected including two DRL algorithms, i.e., DDPG for parameterized action space [31] and DQN, and two non-DRL algorithms, i.e., the myopic and two-stage MPC algorithm [30]. To deploy the DQN and two-stage MPC algorithm, we discretize the action space at a granularity of 20kW, which is the value that achieves the best performance.

TABLE I: Parameters configured in the system model.

Notations	Values	Description
DG model		
D	2	The number of DGs
$P_{\min}^{\mathrm{DG}}$	200kW	The minimum power constraint of a DG
$P_{\max}^{\mathrm{DG}}$	300kW	The maximum power constraint of a DG
Battery model		
$P_{\max}^{\mathrm{E}}$	400kW	The power constraint of the battery
$E_{\max}$	2000kWh	The maximum storage constraint of the battery
$E_{\min}$	24kWh	The minimum storage constraint of the battery
$\eta_{\mathrm{ch}}/\eta_{\mathrm{dis}}$	0.98	The charging/discharging efficiency
Reward function		
a_d	0.005	The quadratic coefficient of cost curve
b_d	6	The monomial coefficient of cost curve
c_d	100	The constant coefficient of cost curve
$C_{\mathrm{R}}/C_{\mathrm{S}}$	25	The fixed running/start-up cost coefficient

We use the real isolated MGs data as the experimental data, where the duration of a time step is set to one hour, i.e., $\Delta_t = 1$, and each data at a time step include two values, representing the average load power and average PV power of the MG system. We regard one-day data, i.e., 24 pieces of data, as one group, i.e., the total number of time steps $T = 24$. The training set consists of the data of seven continuous days. During training, the data for any given day are randomly sampled from these seven days. Besides, the test set is generated by data of the eighth day. This design of data set can prove that the proposed algorithm is not over-fitted and still works after the data set is migrated.

We set up the experimental environment on a Linux server and perform the algorithms in Tensorflow 1.14 using Python. The entire parameters of the system model are listed in Table I, including the parameters of the DG model, battery model and reward function.

B. Experimental Results

1) Performance Across Five Runs: Firstly, Table II summarizes the performance of the proposed HAFH-DDPG and other baseline algorithms respectively. All the DRL models are trained across five runs based on different random seeds to make the results more convincing. We executed one hundred complete episodes of 24 time steps for each algorithm based on the test set, and the performance obtained was the average value of the cumulative rewards in one entire episode. It can be found from Table II that the average performance of the three DRL algorithms across the five runs are better than those of the two non-DRL algorithms. This observation indicates that the DRL algorithms exploit the data to deal with the uncertainty and make more efficient decisions as compared to the two-stage MPC and myopic algorithm. Among the three DRL algorithms, we can observe that the performance of our proposed HAFH-DDPG across the five runs are all larger than those of the other baseline DRL algorithms, which further demonstrates the superiority of HAFH-DDPG. Moreover, the

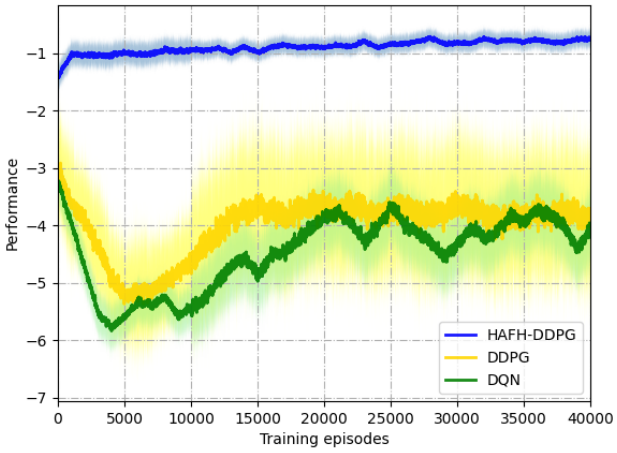

Fig. 2: Average performance of three DRL algorithms across the five runs. The shaded areas show the standard deviation of these algorithms.

average performance of HAFH-DDPG is 30.84% and 30.17% better than those of DDPG and DQN respectively. Finally, it can be found that HAFH-DDPG has the minimal standard deviation among the three DRL algorithms, which shows that this algorithm performs the most stable performance across different runs.

2) Convergence Properties: We focus on the convergence properties of three DRL algorithms across the five runs. As shown in Figure 2, the abscissa is the episode number of training iterations and the ordinate is the average performance of the DDPG, DQN, and HAFH-DDPG algorithms across the five runs. Moreover, the shaded areas indicate the standard deviation of the three algorithms across the five runs. It can be observed that the curve of HAFH-DDPG fluctuates less compared with the other two curves. When the training episodes arrive at approximately 2,000, the convergence goal for HAFH-DDPG has been achieved. In contrast, DDPG and DQN begin to converge at the training episodes of 15,000 and 20,000, respectively. Therefore, HAFH-DDPG algorithm has faster convergence speed than both DDPG and DQN algorithms in the DRL training process. This is because HAFH-DDPG iteratively trains to solve the one-period MDP problems with two adjacent time steps, which is different from DDPG and DQN and makes HAFH-DDPG much easier to converge. Among the three algorithms, it can be observed that the shaded area of HAFH-DDPG is the smallest, which means that the proposed algorithm has more stable performance across different runs than DDPG and DQN.

3) Energy Dispatch Results: The purpose of our proposed algorithm is to learn the best energy management policy for one specific day from the data set. In this case, we observe the UC and ED results of all the DRL and non-DRL algorithms over one day based on the test set. Figure 3 shows the comparison of the load power and generation power trajectories determined by various algorithms. Specifically, the generation power value at each time step is a sum of three parts, i.e., the power of PV, DG and battery.

Firstly, as shown in Figure 3, the generation power curves corresponding to all the DRL algorithms are above the load power curve. On the contrary, for a period of time after 16 p.m., the generated power corresponding to myopic and two-stage MPC algorithms are both less than the load power. This indicates that these two non-DRL algorithms fail to meet the most basic demand of MG, i.e., to ensure the supply-demand balance. The main reason is that these non-DRL algorithms are unable to take full advantage of the battery to charge in advance for the evening peak, which also proves that three DRL algorithms have a certain ability of forward-looking.

In addition, there are salient differences among the three DRL algorithms. Note that both DDPG and DQN maintain the maximum generation power of two ON DGs after 17 p.m., while HAFH-DDPG only outputs the highest generation power from 13 p.m. to 19 p.m. Therefore, compared with DDPG and DQN, HAFH-DDPG can greatly reduce the DG generation cost by turning off one DG after 19 p.m., which means that HAFH-DDPG is undoubtedly a better choice to solve UC problems and save more energy.

VI. Conclusion

In this paper, we have studied how to perform energy management in the MG system, especially focusing on the problem of joint ED and UC. The DRL approach has been adopted to solve this problem and a finite-horizon MDP model has been formulated. Since the DRL approach faces the challenge of high complexity in the discrete-continuous hybrid action space, we have presented the HAFH-DDPG algorithm to address the challenge by breaking the optimization problem down into two steps. In addition, due to the high computation complexity of HAFH-DDPG, the UC action space has been reduced without compromising the optimal performance. The experimental results have demonstrated that our proposed algorithm can achieve better performance than the other benchmark ones.

Appendix A
Proof for Theorem 1

Proof. Our proof is divided into two steps. The first step is to prove that both k^* and k_{m^*} can achieve the maximum immediate reward at any time step t. According to the definitions in (13), (14), and (16), it is obvious that DGs have translatable symmetry for the supply-demand balance cost, power generation cost, and running cost. Therefore, the sum of the three costs is the same for any $k \in \mathcal{A}_m^{\mathrm{UC}}$, i.e.,

$$c_{t,k_1}^{\mathrm{US}} + \sum_{d=1}^{D} (c_{t,k_1}^{\mathrm{DG}_d} + c_{t,k_1}^{\mathrm{R\_DG}_d}) = c_{t,k_2}^{\mathrm{US}} + \sum_{d=1}^{D} (c_{t,k_2}^{\mathrm{DG}_d} + c_{t,k_2}^{\mathrm{R\_DG}_d}), \quad \forall k_1, k_2 \in \mathcal{A}_m^{\mathrm{UC}}. \tag{34}$$

In addition, the DG selection strategy can ensure that the maximum number of ON DGs at time step t are selected to be ON at time step $t+1$. In other words, the strategy minimizes the number of DGs whose $B_t^{\mathrm{DG}_d} = 0$ and $U_t^{\mathrm{DG}_d} = 1$.

TABLE II: Performance after training across the five runs. We present the individual performance of each run for DDPG, DQN, and HAFH-DDPG algorithms. The average performance, best performance, and standard deviation across the five runs are also presented. For comparison, we also include results from the myopic and two-stage MPC algorithms.

Category	Algorithms	Performance							
		Run1	Run2	Run3	Run4	Run5	Average	Best	Std Deviation
non-DRL	myopic	-5.3529							-
	two-stage MPC	-4.5286							-
DRL	DDPG	-3.5815	-3.7223	-3.9206	-4.8374	-4.1853	-4.4094	-3.5815	0.4955
	DQN	-4.1698	-3.6735	-3.8928	-4.2006	-3.7248	-3.9323	-3.6735	0.2450
	HAFH-DDPG	-2.7581	-2.7142	-2.5263	-2.8609	-2.4514	-2.6622	-2.4514	0.1690

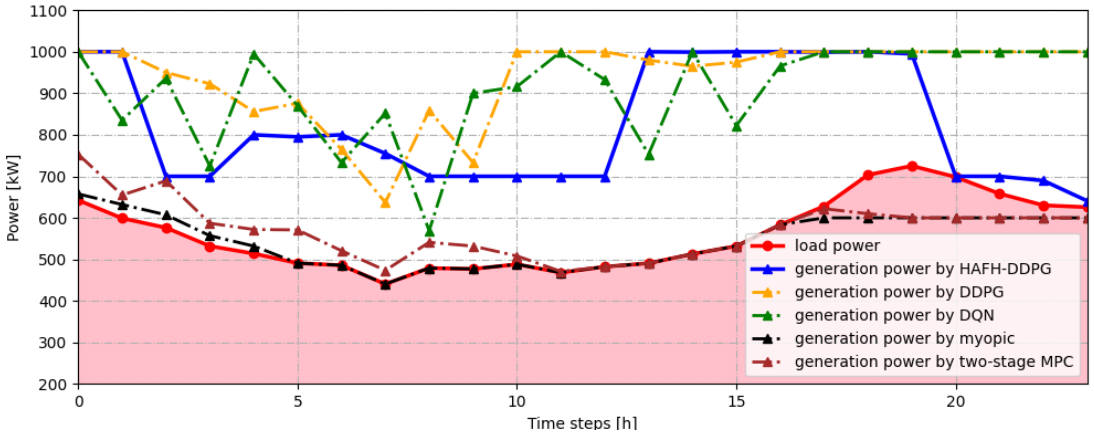

Fig. 3: Comparison of the load and generation power trajectories determined by various algorithms for a specific test episode.

According to (1) and (15), the DG selection strategy in (31) leads to the UC action k_m in $\mathcal{A}_m^{\mathrm{UC}}$ that minimizes the start-up cost, i.e.,

$$k_m = \arg\min_{k \in \mathcal{A}_m^{\mathrm{UC}}} \left(\sum_{d=1}^{D} c_{t,k}^{\mathrm{S\_DG}_d} \right). \tag{35}$$

Therefore, according to the reward definition in (12), k_m derived from the strategy maximizes the reward according to (34) and (35), i.e.,

$$k_m = \arg\max_{k \in \mathcal{A}_m^{\mathrm{UC}}} \left(r(S_t, k, a_k^{\mathrm{ED}^*}) \right). \tag{36}$$

Thus, we can derive

$$\begin{aligned} \max_{k \in \mathcal{A}^{\mathrm{UC}}} \left(r(S_t, k, a_k^{\mathrm{ED}^*}) \right) &\overset{(a)}{=} \max_{m \in \hat{\mathcal{A}}^{\mathrm{UC}}} \max_{k \in \mathcal{A}_m^{\mathrm{UC}}} \left(r(S_t, k, a_k^{\mathrm{ED}^*}) \right) \\ &\overset{(b)}{=} \max_{m \in \hat{\mathcal{A}}^{\mathrm{UC}}} \left(r(S_t, k_m, a_{k_m}^{\mathrm{ED}^*}) \right), \end{aligned} \tag{37}$$

where (a) is due to (30); and (b) follows from (36).

In the second step, we prove (33) using induction by the Bellman equation (23). For the last time step T, we have

$$Q_T \left(S_T, k, a_k^{\mathrm{ED}^*} \right) = r \left(S_T, k, a_k^{\mathrm{ED}^*} \right), \forall k \in \mathcal{A}^{\mathrm{UC}} \tag{38}$$

Thus, combining (37) and (38), we have

$$\max_{m \in \hat{\mathcal{A}}^{\mathrm{UC}}} Q_T \left(S_T, k_m, a_{k_m}^{\mathrm{ED}^*} \right) = \max_{k \in \mathcal{A}^{\mathrm{UC}}} Q_T \left(S_T, k, a_k^{\mathrm{ED}^*} \right). \tag{39}$$

Then, we assume that

$$\begin{aligned} &\max_{m' \in \hat{\mathcal{A}}^{\mathrm{UC}}} Q_{t+1} \left(S_{t+1}, k_{m'}, a_{k_{m'}}^{\mathrm{ED}^*} \right) = \\ &\max_{k' \in \mathcal{A}^{\mathrm{UC}}} Q_{t+1} \left(S_{t+1}, k', a_{k'}^{\mathrm{ED}^*} \right), \forall S_{t+1} \in \mathcal{S}. \end{aligned} \tag{40}$$

Next, we can prove

$$\begin{aligned} &\sum_{S_{t+1} \in \mathcal{S}} \Pr \left(S_{t+1} | S_t, k_1, a_{k_1}^{\mathrm{ED}^*} \right) \cdot \max_{k' \in \mathcal{A}^{\mathrm{UC}}} Q_t \left(S_{t+1}, k', a_{k'}^{\mathrm{ED}^*} \right) \\ &= \sum_{S_{t+1} \in \mathcal{S}} \Pr \left(S_{t+1} | S_t, k_2, a_{k_2}^{\mathrm{ED}^*} \right) \cdot \max_{k' \in \mathcal{A}^{\mathrm{UC}}} Q_t \left(S_{t+1}, k', a_{k'}^{\mathrm{ED}^*} \right), \\ &\forall k_1, k_2 \in \mathcal{A}_m^{\mathrm{UC}}. \end{aligned} \tag{41}$$

This is because the next state S_{t+1} consists of four parts, where the load and PV at the next step time $t+1$, i.e., P_{t+1}^{L} and P_{t+1}^{PV}, do not depend on the UC action k. Moreover, all the UC actions $\forall k \in \mathcal{A}_m^{\mathrm{UC}}$ lead to the same SoC state E_{t+1} according to (4), (5), (6) and (9). Finally, the next switching state B_{t+1} are different for $\forall k \in \mathcal{A}_m^{\mathrm{UC}}$, but the number of ON DGs at the next time step $t+1$ are the same, i.e., m. Therefore, based on mathematical induction, (41) is proved.

Finally, we can prove (33) at each time step t by considering the following Bellman equations based on (23), i.e.,

$$\begin{aligned} \max_{m \in \hat{\mathcal{A}}^{\mathrm{UC}}} Q_t \left(S_t, k_m, a_{k_m}^{\mathrm{ED}^*} \right) &\overset{(a)}{=} \max_{m \in \hat{\mathcal{A}}^{\mathrm{UC}}} \Big\{ r(S_t, k_m, a_{k_m}^{\mathrm{ED}^*}) + \\ &\mathbb{E}_{S_{t+1}} \left[\gamma \cdot \max_{m' \in \hat{\mathcal{A}}^{\mathrm{UC}}} Q_t \left(S_{t+1}, k_{m'}, a_{k_{m'}}^{\mathrm{ED}^*} \right) | S_t, k_m, a_{k_m}^{\mathrm{ED}^*} \right] \Big\} \end{aligned}$$

$$
\begin{aligned}
&\overset{(b)}{=} \max_{m\in\hat{\mathcal{A}}^{\mathrm{UC}}} \Big\{ r(S_t, k_m, a_{k_m}^{\mathrm{ED}^*}) + \\
&\mathop{\mathbb{E}}_{S_{t+1}} \left[\gamma \cdot \max_{k'\in\mathcal{A}^{\mathrm{UC}}} Q_t \left(S_{t+1}, k', a_{k'}^{\mathrm{ED}^*} \right) | S_t, k_m, a_{k_m}^{\mathrm{ED}^*} \right] \Big\} \\
&\overset{(c)}{=} \max_{m\in\hat{\mathcal{A}}^{\mathrm{UC}}} \max_{k\in\mathcal{A}_m^{\mathrm{UC}}} \Big\{ r(S_t, k, a_k^{\mathrm{ED}^*}) + \\
&\mathop{\mathbb{E}}_{S_{t+1}} \left[\gamma \cdot \max_{k'\in\mathcal{A}^{\mathrm{UC}}} Q_t \left(S_{t+1}, k', a_{k'}^{\mathrm{ED}^*} \right) | S_t, k, a_k^{\mathrm{ED}^*} \right] \Big\} \\
&\overset{(d)}{=} \max_{k\in\mathcal{A}^{\mathrm{UC}}} \Big\{ r(S_t, k, a_k^{\mathrm{ED}^*}) + \\
&\mathop{\mathbb{E}}_{S_{t+1}} \left[\gamma \cdot \max_{k'\in\mathcal{A}^{\mathrm{UC}}} Q_t \left(S_{t+1}, k', a_{k'}^{\mathrm{ED}^*} \right) | S_t, k, a_k^{\mathrm{ED}^*} \right] \Big\} \\
&\overset{(e)}{=} \max_{k\in\mathcal{A}^{\mathrm{UC}}} Q_t \left(S_t, k, a_k^{\mathrm{ED}^*} \right).
\end{aligned} \tag{42}
$$

where (a) and (e) are due to the definition of Bellman equation; (b) follows by (40); (c) is due to (41) and the definition of expectation; (d) follows by (30). Therefore, (33) in Theorem 1 is proved according to (42).

□

REFERENCES

[1] H. Shuai, F. Li, H. Pulgar-Painemal, and Y. Xue, "Branching dueling q-network-based online scheduling of a microgrid with distributed energy storage systems," *IEEE Transactions on Smart Grid*, vol. 12, no. 6, pp. 5479–5482, 2021.

[2] E. Mocanu, D. C. Mocanu, P. H. Nguyen, A. Liotta, M. E. Webber, M. Gibescu, and J. G. Slootweg, "On-line building energy optimization using deep reinforcement learning," *IEEE Transactions on Smart Grid*, vol. 10, no. 4, pp. 3698–3708, 2019.

[3] M. Azaroual, M. Ouassaid, and M. Maaroufi, "Optimal control for energy dispatch of a smart grid tied pv-wind-battery hybrid power system," in *2019 Third International Conference on Intelligent Computing in Data Sciences (ICDS)*. IEEE, 2019, pp. 1–7.

[4] G. van Leeuwen, T. AlSkaif, M. Gibescu, and W. van Sark, "An integrated blockchain-based energy management platform with bilateral trading for microgrid communities," *Applied Energy*, vol. 263, p. 114613, 2020. [Online]. Available: https://www.sciencedirect.com/science/article/pii/S0306261920301252

[5] H. Çimen, N. Çetinkaya, J. C. Vasquez, and J. M. Guerrero, "A microgrid energy management system based on non-intrusive load monitoring via multitask learning," *IEEE Transactions on Smart Grid*, vol. 12, no. 2, pp. 977–987, 2020.

[6] A. Bhardwaj, V. K. Kamboj, V. K. Shukla, B. Singh, and P. Khurana, "Unit commitment in electrical power system-a literature review," in *2012 IEEE International Power Engineering and Optimization Conference Melaka, Malaysia*, 2012, pp. 275–280.

[7] B. O'Donoghue, I. Osband, R. Munos, and V. Mnih, "The uncertainty bellman equation and exploration," in *International Conference on Machine Learning*, 2018, pp. 3836–3845.

[8] E. Mocanu, D. C. Mocanu, P. H. Nguyen, A. Liotta, M. E. Webber, M. Gibescu, and J. G. Slootweg, "On-line building energy optimization using deep reinforcement learning," *IEEE transactions on smart grid*, vol. 10, no. 4, pp. 3698–3708, 2018.

[9] C.-L. Tseng, *On power system generation unit commitment problems*. University of California, Berkeley, 1996.

[10] C.-A. Li, R. B. Johnson, and A. J. Svoboda, "A new unit commitment method," *IEEE Transactions on Power Systems*, vol. 12, no. 1, pp. 113–119, 1997.

[11] W. B. Powell and S. Meisel, "Tutorial on stochastic optimization in energy—part ii: An energy storage illustration," *IEEE Transactions on Power Systems*, vol. 31, no. 2, pp. 1468–1475, 2015.

[12] J. P. Catalão, *Smart and sustainable power systems: operations, planning, and economics of insular electricity grids*. CRC Press, 2017.

[13] M. P. Nowak and W. Römisch, "Stochastic lagrangian relaxation applied to power scheduling in a hydro-thermal system under uncertainty," *Annals of Operations Research*, vol. 100, no. 1, pp. 251–272, 2000.

[14] S. Takriti, J. R. Birge, and E. Long, "A stochastic model for the unit commitment problem," *IEEE Transactions on Power Systems*, vol. 11, no. 3, pp. 1497–1508, 1996.

[15] P. Carpentier, G. Gohen, J.-C. Culioli, and A. Renaud, "Stochastic optimization of unit commitment: a new decomposition framework," *IEEE Transactions on Power Systems*, vol. 11, no. 2, pp. 1067–1073, 1996.

[16] A. Tuohy, P. Meibom, E. Denny, and M. O'Malley, "Unit commitment for systems with significant wind penetration," *IEEE Transactions on power systems*, vol. 24, no. 2, pp. 592–601, 2009.

[17] S. Takriti, B. Krasenbrink, and L. S.-Y. Wu, "Incorporating fuel constraints and electricity spot prices into the stochastic unit commitment problem," *Operations Research*, vol. 48, no. 2, pp. 268–280, 2000.

[18] M. A. Velasquez, J. Barreiro-Gomez, N. Quijano, A. I. Cadena, and M. Shahidehpour, "Intra-hour microgrid economic dispatch based on model predictive control," *IEEE Transactions on Smart Grid*, vol. 11, no. 3, pp. 1968–1979, 2019.

[19] L. Yu, S. Qin, M. Zhang, C. Shen, T. Jiang, and X. Guan, "A review of deep reinforcement learning for smart building energy management," *IEEE Internet of Things Journal*, vol. 8, no. 15, pp. 12 046–12 063, 2021.

[20] S. Nagarathinam, V. Menon, A. Vasan, and A. Sivasubramaniam, "Marco-multi-agent reinforcement learning based control of building hvac systems," in *Proceedings of the Eleventh ACM International Conference on Future Energy Systems*, 2020, pp. 57–67.

[21] Y. Yang, J. Hao, Y. Zheng, X. Hao, and B. Fu, "Large-scale home energy management using entropy-based collective multiagent reinforcement learning framework," in *Proceedings of the 18th International Conference on Autonomous Agents and MultiAgent Systems*, 2019, pp. 2285–2287.

[22] S. Lee and D.-H. Choi, "Energy management of smart home with home appliances, energy storage system and electric vehicle: A hierarchical deep reinforcement learning approach," *Sensors*, vol. 20, no. 7, p. 2157, 2020.

[23] X. Zhang, D. Biagioni, M. Cai, P. Graf, and S. Rahman, "An edge-cloud integrated solution for buildings demand response using reinforcement learning," *IEEE Transactions on Smart Grid*, vol. 12, no. 1, pp. 420–431, 2020.

[24] L. Yu, W. Xie, D. Xie, Y. Zou, D. Zhang, Z. Sun, L. Zhang, Y. Zhang, and T. Jiang, "Deep reinforcement learning for smart home energy management," *IEEE Internet of Things Journal*, vol. 7, no. 4, pp. 2751–2762, 2019.

[25] V. François-Lavet, D. Taralla, D. Ernst, and R. Fonteneau, "Deep reinforcement learning solutions for energy microgrids management," in *European Workshop on Reinforcement Learning (EWRL 2016)*, 2016.

[26] Y. Ji, J. Wang, J. Xu, X. Fang, and H. Zhang, "Real-time energy management of a microgrid using deep reinforcement learning," *Energies*, vol. 12, no. 12, 2019. [Online]. Available: https://www.mdpi.com/1996-1073/12/12/2291

[27] F. Wei, Z. Wan, and H. He, "Cyber-attack recovery strategy for smart grid based on deep reinforcement learning," *IEEE Transactions on Smart Grid*, vol. 11, no. 3, pp. 2476–2486, 2020.

[28] L. Lei, Y. Tan, G. Dahlenburg, W. Xiang, and K. Zheng, "Dynamic energy dispatch based on deep reinforcement learning in iot-driven smart isolated microgrids," *IEEE Internet of Things Journal*, vol. 8, no. 10, pp. 7938–7953, May 2021.

[29] H. Shuai and H. He, "Online scheduling of a residential microgrid via monte-carlo tree search and a learned model," *IEEE Transactions on Smart Grid*, vol. 12, no. 2, pp. 1073–1087, 2020.

[30] J. Sachs and O. Sawodny, "A two-stage model predictive control strategy for economic diesel-pv-battery island microgrid operation in rural areas," *IEEE Transactions on Sustainable Energy*, vol. 7, no. 3, pp. 903–913, 2016.

[31] M. Hausknecht and P. Stone, "Deep reinforcement learning in parameterized action space," 2016.

[32] J. Xiong, Q. Wang, Z. Yang, P. Sun, L. Han, Y. Zheng, H. Fu, T. Zhang, J. Liu, and H. Liu, "Parametrized deep q-networks learning: Reinforcement learning with discrete-continuous hybrid action space," *arXiv preprint arXiv:1810.06394*, 2018.

[33] M. Wu, Y. Gao, A. Jung, Q. Zhang, and S. Du, "The actor-dueling-critic method for reinforcement learning," *Sensors*, vol. 19, no. 7, p. 1547, 2019.

[34] D. Silver, G. Lever, N. Heess, T. Degris, D. Wierstra, and M. Riedmiller, "Deterministic policy gradient algorithms," in *International conference on machine learning*. PMLR, 2014, pp. 387–395.